SLAC-PUB-17349

Trapping of charged and dust particles in the RF field of a superconducting cavity

Alexander Novokhatski* and Sam Heifets
SLAC National Accelerator Laboratory, Menlo Park, CA 94025, USA

Abstract

We suggest an explanation of the observations of the glowing filaments in a superconducting cavity. We show that the motion of a charged particle in a multi-cell RF cavity and of a dust particle in a single-cell RF cavity can be stable. The analysis of stability is illustrated by numerical calculations. This effect may also explain the possible failure of high gradient tests of superconducting cavities, which are planned to be used in the linear accelerators for XFEL.

1 Introduction

In this paper, we study the stability of the motion of charged particles and dust particles in a single-cell and multi-cell RF cavity. The paper is inspired by the observation of light emitting filaments during the power test of the niobium superconducting cavities [1]. The glowing filament of light was observed by a CCD camera installed at the end of a single-cell 1500 MHz cavity when operating the cavity in field emission regime. The cavity gradients during these filament events were 2-4 MV/m. Similar light emission filaments were observed at the center of a 5-cell SC cavity at 4.4 MV/m, trapped by RF fields in closed-orbit trajectories. The filaments appear at the beginning of the field emission, lasted a few seconds, and then followed by a flash of light and drop of the cavity Q-factor. After that when the gradient was reduced, and a new run was started no events were detected and the Q value was at the highest level. The authors conclude that it was conceivable that filaments are due to charged particles generated by the field emission and trapped in the RF field. The glow could be due to light emission, or ionization of residual helium gas. However, at that time it was not obvious that particles can be trapped in RF fields on the stable closed trajectories that were observed in experiments.

*novo@slac.stanford.edu

This material is based upon work supported by the U.S. Department of Energy,
Office of Science, under Contract No. DE-AC02-76SF00515.

This phenomenon may also be due to sudden drops of the beam life time at the Beijing Collider (BEPC). The events had typical features of dust events [7], [8], [9]: they happened randomly in a wide range of the electron beam current, both in single-bunch and multi-bunch regimes. They were not reproducible with the same machine parameters and never happened with a positron beam. It was noticed [10] that the lifetime can be restored by changing the voltage of cavities. However, the reason for this was not clear.

It is well known that a charged particle can be trapped by electro-magnetic (EM) fields. The Penning trap used DC EM fields while the Paul trap is based on a combination of DC and AC fields. The problem of possible potential wells for charged particles in a high frequency azimuthally symmetric field was analyzed in Ref. [2].

Trapping in an RF cavity was discussed for a rectangular box cavity [3]. We include discussion of such trapping in the first section of the paper for completeness. An electromagnetic field in a cavity is a superposition of the fields of the RF modes, which can be excited by the beam or external generator. Main mode is usually used for the particle acceleration. Although an accelerating mode of a single-cell RF cavity cannot trap a charged particle, we emphasize that the trapping is possible in a multi-cell superconducting cavity used in the accelerating structures of linear accelerators.

However, we believe that the light emitting filaments can be explained not only by the trapping of the charged particles but also by trapping of dust particles. A small particle model as a possible explanation of cavity lights was discussed in reference [4] and reference [5].The conclusion was that spheres of any known material cannot, in this model, explain the observations. However, we made very careful analysis of the forces acting on a dust particle and found out that the trajectory of a dust particle can be stable. In the second part of the paper we show that a dust particle can be stable in a single RF cavity of a spherical shape. We believe that the dust particles trapped in the RF cavity can provide also an explanation for Beijing observations because the trajectory of a trapped particle in our model substantially depends on the cavity voltage. Finally, in conclusion, we discuss and summarize results.

2 Charged particle in the RF field

Let us study the motion of a charged particle in the RF field of a multi-cell cavity near a cavity iris. Suppose that the cavity is cylindrically symmetric, and the field corresponds to the azimuthally symmetrical mode. Using the cylindrical coordinate system (r, ϕ, z) with the z axis along the resonator axes (the direction of the beam propagation), we can expand the nonzero components of the field,

$$E_r(r,z) = -E_0\{\frac{r}{2a} - \frac{r^3}{16a}(\frac{\omega}{c})^2 + ...\}$$
$$E_z(r,z) = E_0\{\frac{z}{a} - \frac{zr^2}{4a}(\frac{\omega}{c})^2\}$$

$$H_\phi(r,z) = E_0 \frac{i}{2}(\frac{\omega}{c})\frac{rz}{a} + ... \tag{1}$$

Here E_0 is the amplitude of the RF accelerating mode with the frequency ω, and the factor $e^{-i\omega t}$ implies time dependence. E_z field is equal to zero in the center of the iris ($z = 0$) and approaching the value of the accelerating field E_0 at the distance a from the iris center. The characteristic length a is of the order of the radius of the iris. The field 1 satisfies Maxwell equations with the accuracy of the neglected terms.

Assuming that $eE_0 a \ll mc^2(\frac{\omega}{c}a)$, then the magnetic force can be neglected. The nonlinear terms are negligible for small $r/a \ll 1$, $z/a \ll 1$.

The Lorentz force has only (r, z) components, therefore the angular momentum $L = mr^2\dot{\phi}$ is a constant of motion. The remaining equations of motion for a non-relativistic particle with the charge e and mass m in the linear approximation take the form

$$\begin{aligned} m\ddot{r} &= f_r(r)\cos(\omega t) + \frac{L^2}{mr^3}, \quad f_r(r) = -eE_0\,\frac{r}{2a} \\ m\ddot{z} &= f_z(z), \quad f_z(z) = eE_0\,\frac{z}{a}\cos(\omega t) \end{aligned} \tag{2}$$

A solution can be found as the sum of a slow $\bar{r}$ and small but fast $\tilde{r}$ varying terms, $r = \bar{r} + \tilde{r}$, $z = \bar{z} + \tilde{z}$. The equation for the slow motion is obtained by averaging the fast oscillating terms. The equation for the radial motion takes the form

$$m\ddot{\bar{r}} = \frac{L^2}{m\bar{r}^3} + F(\bar{r}) \tag{3}$$

where the radial ponderomotive force

$$F(\bar{r}) = \frac{\partial}{\partial\bar{r}}(\frac{f_r(\bar{r})}{2m\omega})^2 \tag{4}$$

The first term $L^2/m\bar{r}^3$ in Eq. (3) describes the centrifugal barrier and, for $L \neq 0$, prevents a particle to go to the axes $r \to 0$. One can find similarity of this force with the Miller force [6]

To have a bounded motion at large $\bar{r}$, the second term at large $\bar{r}$ has to be negative. That is possible for $\bar{r} > r_s = (3L^2/\omega^2)^{1/4}$. Assuming that $\bar{r} >> r_s$, we get

$$F(\bar{r}) = \frac{L^2}{\bar{r}^3} - \Omega_r^2\bar{r}. \tag{5}$$

We assume that the field is low, $(eE_0/m\omega^2 a) << 1$. Then, the equilibrium radius is

$$r_{eq}^4 = 2(\frac{2L\omega a}{eE_0})^2. \tag{6}$$

Small oscillations around r_{eq} are stable and have frequency

$$\Omega_r = \frac{1}{\sqrt{2}}\,(\frac{eE_0}{ma\omega}). \tag{7}$$

Similarly, small longitudinal oscillation around the equilibrium point $z = 0$ has a frequency

$$\Omega_z = \frac{1}{\sqrt{2}}\,(\frac{eE_0}{m\omega a}) \tag{8}$$

equal to the frequency of radial oscillations.

For the low field $\Omega_r << \omega$, i.e. that frequency of oscillations is slow compared to the RF frequency. That is also consistent with the assumption that the motion can be separated into slow and fast parts.

The initial conditions $r(0) = r_{eq}$, $z(0) = \dot{z}(0) = \dot{r}(0) = 0$ correspond to the motion on the circle r_{eq} with the azimuthal angular velocity $\dot{\phi} = \Omega_\phi$,

$$\Omega_\phi = \frac{L}{mr_{eq}^2} = \frac{\Omega_r}{2}. \tag{9}$$

Hence, the frequency of the radial oscillations is two times the azimuthal frequency. If the amplitude of the radial oscillation around r_{eq} is δr, the horizontal coordinate of a particle

$$x(t) = (r_{eq} + \delta r \cos(2\Omega_\phi t))\,\cos(\Omega_\phi t), \tag{10}$$

and the trajectory in (x, y) plane is an ellipse.

If the particle starts at the iris wall $r \simeq a$ with the angular velocity $\dot{\phi}_0$, then $L = ma^2\dot{\phi}_0$ and initial velocity $v(0) \simeq a\dot{\phi}_0$. Then, $r_{eq} < a$ for a sufficiently large field,

$$(\frac{eE_0}{m\omega}) > v_0. \tag{11}$$

Condition Eq. (11) means that the velocity acquired by a particle in a half of the RF period is large compared to the initial velocity.

As an example, we choose the TM mode of a pill-box cavity $0 \le r \le b$, $0 \le z \le l$. The non-zero components of the field are

$$\begin{aligned}
E_r &= E_0\,\frac{\pi b}{\nu l}\,J_1(\frac{\nu r}{b})\,\sin(\frac{\pi z}{l})\,\cos(\omega t),\\
E_z &= E_0\,J_0(\frac{\nu r}{b})\,\cos(\frac{\pi z}{l})\,\cos(\omega t),\\
H_\phi &= -E_0\,\frac{\omega b}{\nu c}J_1(\frac{\nu r}{b})\,\cos(\frac{\pi z}{l})\,\sin(\omega t).
\end{aligned} \tag{12}$$

Here, $\omega/c = \sqrt{(\pi/l)^2 + (\nu/b)^2}$ is the mode frequency, $\nu \simeq 2.405$ is the first root of $J_0(\nu) = 0$, and E_0 is the accelerating gradient. The mode has a node at $z = l/2$.

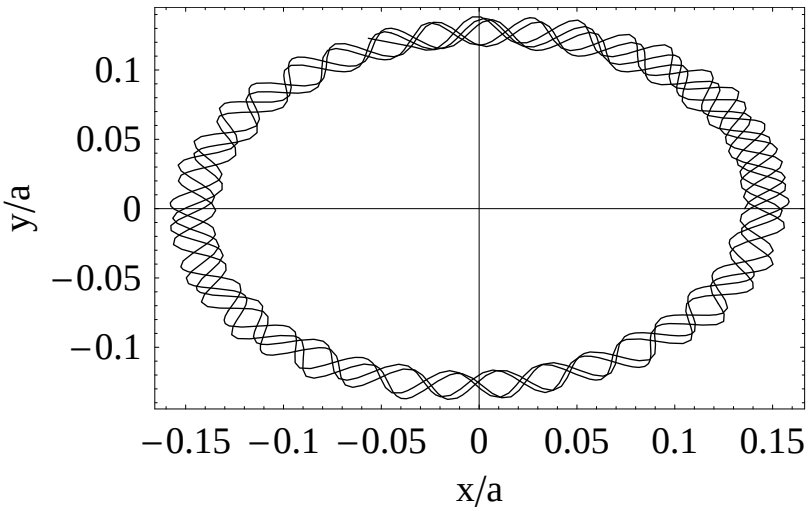

Figure 1: Trajectory in (x,y) plane with initial conditions corresponding to the equilibrium $r(0) = r_{eq}$, see text. Parameters $\lambda = 0.05$, $\mu = 1.0\,10^{-3}$, $\omega t_{max} = 500$.

As above, the quantity $L = mr^2\dot{\phi}$ is a constant of motion. We define the quantity $\dot{\phi}(0)$ by $L = ma^2\dot{\phi}(0)$ and use notation $\mu = \dot{\phi}(0)/\omega$. The equilibrium radius in this case is

$$\frac{r_{eq}}{b} = (\frac{8\mu^2}{(\pi\lambda)^2})^{1/4}, \tag{13}$$

where

$$\lambda = \frac{eE_0 l}{mc^2(\omega l/c)^2}. \tag{14}$$

and we assumed the low field, $2\mu\nu^2 < \pi\lambda << 1$.

Small radial and longitudinal oscillations around the equilibrium are stable and have frequency

$$\Omega = \frac{\pi\lambda}{\sqrt{2}}. \tag{15}$$

We compared the estimates with results of numeric integration of exact equations of motion. Fig. (1) shows the trajectory in (x, y) plane for the initial conditions corresponding to the equilibrium: $r(0) = r_{eq}$, $z(0)/l = 1/2$, $\dot{z}(0) = \dot{r}(0) = 0$, where $r_{eq}/b = 0.1357$ is given by numeric solution. Small oscillations around a circle are due to higher harmonics 2ω, 3ω.

2.1 A multi-cell cavity

Usually, the accelerating mode of a single cell cavity does not have nodes and trapping of a charged particle does not take place. However, in a multi-cell cavity a charged particle can have a stable trajectory. To verify this possibility, we calculate particle trajectories in the CEBAF 5-cell cavity [1]. We include all field components in computer simulations. The geometry of an iris and longitudinal eclectic field distributions at different radial positions is shown in Fig. 2. The aperture of the structure is 3.5 cm. The fields are normalized to 4 MeV/m accelerating gradient (including time-flight effect). To calculate these fields we used a computer code, which is described in the reference [11]. According to calculations, the electric field on the surface of irises is not much smaller than the field on the axes, and any local enhancement in the real cavity due to roughness or electron emission can change the field distribution.

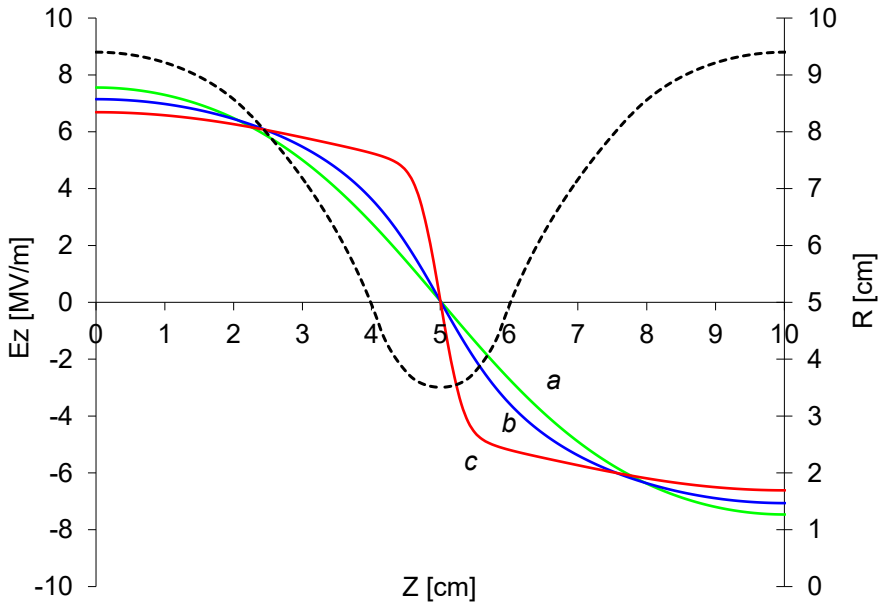

Figure 2: Geometry of an iris of a CEBAF multi-cell cavity (gray line). Longitudinal electric field at a different radial position: $r = 0$ cm (green line), $r = 2.5$ cm (blue line), $r = 3.45$ cm (red line). Fields are normalized to 4 MeV/m accelerating gradient.

We found stable trajectories of charged particles located under the iris. A typical trajectory is an ellipse, which is rotating in time in azimuthal direction. Fig. 3 shows the trajectory on x-y plain and z-y plain. In this simulation, we obtained a revolution frequency of 40 Hz for a mass of a charged particle of $4 \cdot 10^8$ MeV. Each revolution turn corresponds to $3.5 \cdot 10^7$ periods of the RF field. The initial radial position is 2 cm and the azimuthal momentum is 2 MeV. With the zero initial conditions $r(0) = r_{eq}$, $z(0) = z_{eq}$, $\dot{r}(0) = \dot{z}(0) = 0$, an elliptical shape of trajectories becomes a circular. Trajectory stays still almost circular even in the case of longitudinal oscillations. Fig. 4 shows this case.

The initial azimuthal momentum takes the optimum value of 7.5 MeV for the radius of 2 cm, when the initial longitudinal position is offset from the center of an iris to 1 mm.

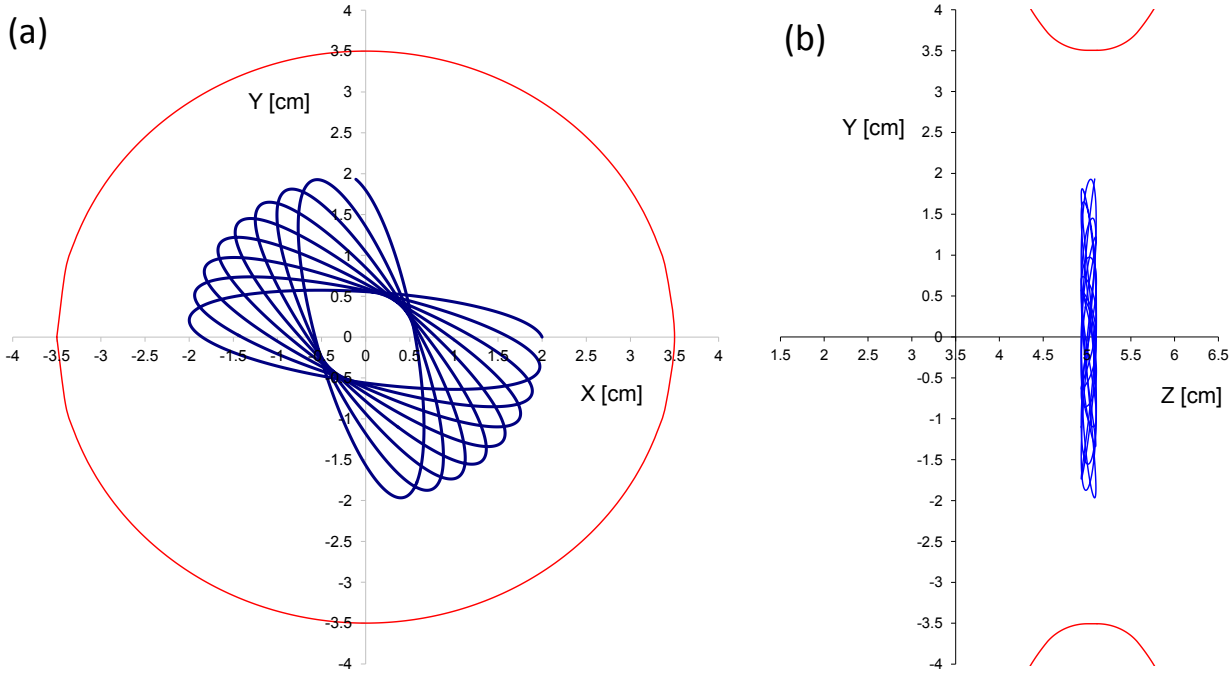

Figure 3: Charged particle trajectory. (a) Projection on x-y plane and (b) projection z-y plane. Red line shows the aperture and shape of an iris.

3 Dust stability

As shown above, a charged particle can be stable in RF field of a multi-cell cavity in the vicinity of irises. To produce visible light, a particle has to be macroscopic and radiate thermally or in the collisions with the residual gas. From the study of dust particles [7], [8], [9], it is known that a dust particle with the radius of the order of 1 μm and the mass $M \simeq 10^{12}$ of the proton mass, can be stable for macroscopic time and acquire charge Qe interacting with the beam up to $Q/e \simeq 10^8$. There is no doubt that a dust particle in the RF cavity would be charged even without a beam by the field emitted electrons and can be heated by the flux of the field emitted electrons from the walls of the cavity or from ohmic heating of the conductive dust particle.

The ponderomotive force for a single-cell cavity does not lead to trapping. Because the RF field $E_{rf}(z)$ in the center of such a cavity has a maximum, the ponderomotive force can not provide particle stability. On top of that, the magnitude of the force for a micron size of a particle is weak for the RF gradient of the order of $E_{rf} \simeq 1 MeV/m$.

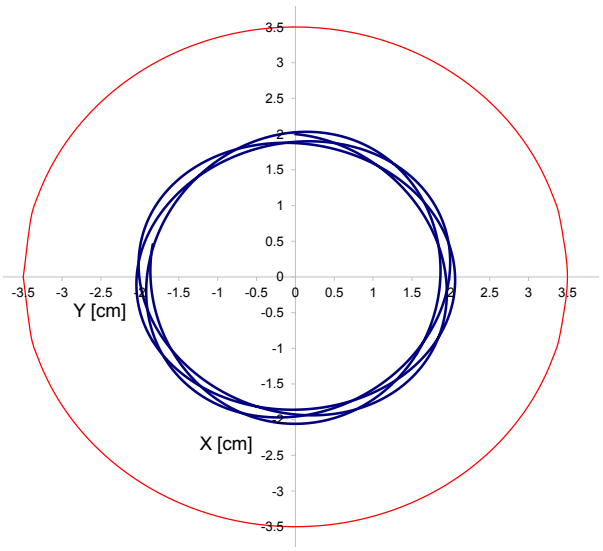

Figure 4: Almost circular charged particle trajectory in presents of longitudinal oscillations.

Another force acting on the dust particle is related to the electric and magnetic polarizabilities of the particle. Although expressions for polarizabilities of a spherical particle in a uniform external field are well known, we need to carefully study the effect of the non-uniformity of the field of the cavity.

We consider here the stability of a round dust particle in a spherical RF cavity with the conductivity σ and $\mu = 1$. We denote the radii of the cavity and the dust particle by b and a_d respectively. Naturally $a_d << b$. We allow an arbitrary ratio of the skin depth δ to a_d.

The force acting on the dust particle is defined by the integral [13] over the surface of the dust particle,

$$F_i = \int \frac{dS}{8\pi} \hat{r}_j [\mathrm{E}_i \mathrm{D}_j + \mathrm{D}_i \mathrm{E}_j - \delta_{i,j} \mathrm{E.D} + (\mathrm{E}, \mathrm{D}) \rightarrow (\mathrm{H}, \mathrm{B})], \tag{16}$$

where the unit radial vector $\hat{r}$ is normal to the surface and directed outside of the particle. The fields are given in terms of the Fourier components E defined as $\mathrm{E}(t) = (1/2)(E\, e^{-i\omega_0 t} + c.c.)$. The average over time force is given by Eq. (16) where quadratic in E, H terms should be replaced by $(1/4)(EE^* + c.c.)$. E and H are the Fourier components of EM fields on the surface of the particle, and $D = (k_0^2 + 2i/\delta^2)E$, where δ is the skin depth at the frequency $\omega_0 = k_0 c$. The magnetic terms are obtained replacing both E and D by H (assuming $\mu = 1$). The field outside the particle is given by the sum of the RF field E_{cav}, H_{cav} and the field E_{ind}, H_{ind} induced by the particle. The fields inside of the particle are the induced fields. The RF cavity field itself does not contribute to the force acting on a dust particle (see Appendix 2).

The global spherical coordinate system (c.s.) with the origin at the cavity center is defined by the polar axes $\hat{z}$ along the beam line and the orthogonal set of unit vectors $(\hat{R}, \hat{\alpha}, \hat{\phi})$. In this basis, the Fourier harmonics E_{cav}, H_{cav} of the lowest accelerating TM mode of the cavity at the point with the spherical coordinates R, α, ϕ are

$$H_{cav} = -\frac{3E_0}{2}\{0,\, 0,\, (\frac{\cos\mu}{\mu} - \frac{\sin\mu}{\mu^2})\,\sin\alpha\},$$
$$E_{cav} = \frac{-3iE_0}{2}\{\frac{2(\mu\cos\mu - \sin\mu)}{\mu^3}\cos\alpha,\, \frac{\mu\cos\mu + (\mu^2-1)\sin\mu}{\mu^3}\,\sin\alpha,\, 0\}, \quad (17)$$

where $\mu = k_0 R$ and $k_0 = \omega_0/c$. The mode frequency ω_0 is given by $\mu_0 = k_0 b = 2.74371..$, and the accelerating field $E_z(0) = E_0$ at $R = 0$.

It is convenient to describe the induced field in the local c.s. with the origin at the center of the dust particle. The local Cartesian c.s. can be defined by the unit orthogonal vectors ξ, η, ζ oriented along the unit vectors of the global spherical c.s.

$$\hat{\xi} = \hat{R}, \quad \hat{\eta} = \hat{\phi}, \quad \hat{\zeta} = -\hat{\alpha}. \quad (18)$$

The local unit vectors of the spherical c.s. $\{\hat{r}, \hat{\beta}, \hat{\psi}\}$ with the polar axes along $\hat{\zeta}$ is related to the Cartesian unit vectors $\hat{\xi}, \hat{\eta}, \hat{\zeta}$ by

$$\hat{r} = \hat{\xi}\sin\beta\cos\psi + \hat{\eta}\sin\beta\sin\psi + \hat{\zeta}\cos\beta,$$
$$\hat{\beta} = \hat{\xi}\cos\beta\cos\psi + \hat{\eta}\cos\beta\sin\psi - \zeta\sin\beta,$$
$$\hat{\psi} = -\hat{\xi}\sin\psi + \hat{\eta}\cos\psi. \quad (19)$$

In particular, $\hat{z} = \hat{\xi}\cos\alpha + \hat{\zeta}\sin\alpha$, and the unit radius vector $\hat{\xi}$ in the local spherical c.s. is

$$\hat{\xi} = \hat{r}\sin\beta\cos\psi + \hat{\beta}\cos\beta\cos\psi - \hat{\psi}\sin\psi. \quad (20)$$

It is known that the polarizability of a particle and, consequently the force acting on the particle both are proportional to a_d^3. Because the surface integral Eq. (D1.1) already give the factor a_d^2, it suffices to determine the fields on the surface neglecting terms of the order of a_d^2. The cavity fields on the surface of the particle in the lowest order over the radius $r = a_d$, can be obtained expanding the fields as

$$E_{cav}(\mathbf{R}+\mathbf{r}) = E_{cav}(\mathbf{R}) + (\mathbf{r}.\nabla)E_{cav}(\mathbf{R}), \quad (21)$$

where ∇ denotes the gradient over $\mathbf{R}$.

The same fields in the local c.s. of the dust particle are given by the sum of the TM and TE modes in respect with the radius vector $\mathbf{r}$. The magnetic H^{TM} and electric E^{TM} components of the TM modes are defined [14] by the generating function $\Phi(r, \beta, \psi)$,

$$H^{TM} = \frac{1}{k_0}(\nabla \Phi^{TM} \times \mathbf{r}), \quad E^{TM} = \frac{ik_0}{k^2}(\nabla \times H^{TM}), \tag{22}$$

where $k^2 = k_0^2 + 2i/\delta^2$ and $k = k_0$ inside and outside of the particle, respectively, and $\delta(k_0)$ is the skin depth at the frequency ω_0. The function Φ^{TM} is the solution of the wave equation

$$(\Delta + k^2)\Phi^{TM}(r, \beta, \psi) = 0. \tag{23}$$

The TE modes are defined similarly,

$$E^{TE} = \frac{1}{k_0}(\nabla \Phi^{TE} \times (\mathbf{r})), \quad H^{TE} = -\frac{i}{k_0}(\nabla \times E^{TE}), \tag{24}$$

where Φ^{TE} is also a solution of Eq. (23).

The RF field of the cavity outside of the dust particle is given as superposition of the modes with amplitudes $c_{n,m}$ and $d_{n,m}$ for TM and TE modes, respectively,

$$\begin{aligned} \Phi_{cav}^{TM} &= \sum_{n=0}^{\infty} \sum_{m=-n}^{n} c_{n,m} j^{(+)}[n, k_0 r] P_n^m(\cos\beta) e^{im\psi}, \\ \Phi_{cav}^{TE} &= \sum_{n=0}^{\infty} \sum_{m=-n}^{n} d_{n,m} j^{(+)}[n, k_0 r] P_n^m(\cos\beta) e^{im\psi}. \end{aligned} \tag{25}$$

Here P_n^m are associated Legendre polynomial. The eigen modes inside of the particle should be finite at $r = 0$, and are given in terms of $j[n, kr] = \sqrt{\pi/2kr}\, J_{n+1/2}(kr)$.

The amplitudes $c_{n,m}$ and $d_{n,m}$ can be determined comparing Eq. (21) with Eqs. (22), (24). Because the radial components E_r^{TE} of TE modes and the radial components H_r^{TM} of TM modes are equal to zero, it is convenient for this purpose to compare the radial components,

$$\begin{aligned} E_{cav}^{(r)} &= E_r^{TM} = \frac{i}{k_0 r} \sum n(n+1) c_{n,m} j[n, k_0 r] P_n^m(\cos\beta) e^{im\psi} \\ H_{cav}^{(r)} &= H_r^{TE} = -\frac{i}{k_0 r} \sum n(n+1) d_{n,m} j[n, k_0 r] P_n^m(\cos\beta) e^{im\psi}. \end{aligned} \tag{26}$$

The explicit form of the coefficients $c_{n,m}$ and $d_{n,m}$ is given in the Appendix 1.

The induced field is given in the same way as superposition of the TM and TE modes. We denote the amplitudes of the TM and TE modes induced inside of the particle by κ^{in} and q^{in}, respectively,

$$\Phi_{ind}^{TM} = \sum_{n=0}^{\infty} \sum_{m=-n}^{n} \kappa_{n,m}^{in} j[n,kr] P_n^m(\cos\beta) e^{im\psi},$$
$$\Phi_{ind}^{TE} = \sum_{n=0}^{\infty} \sum_{m=-n}^{n} q_{n,m}^{in} j[n,kr] P_n^m(\cos\beta) e^{im\psi}. \quad (27)$$

The generating functions of the induced fields outside of the particle have a similar to Eqs. (27) structure with $k_{n,m}^{in}$ and $q_{n,m}^{in}$ being replaced by the amplitudes $k_{n,m}^{out}$ and $q_{n,m}^{out}$ and k instead of k_0. The radial functions in the outside region are, generally, a superposition of the Bessel functions, $j[n,kr] = \sqrt{\pi/(2kr)}\, J_{n+1/2}(kr)$ and $j^{(-)}[n,kr] = \sqrt{\pi/(2kr)}\, J_{-n-1/2}(kr)$. The induced modes proportional to $j[n,k_0 r]$ outside of the particle redefine the amplitudes of the rf field. If the amplitude is supported by any feedback system on a constant level, the contribution of such modes is compensated, and the induced field is given as a superposition of terms proportional to $j^{(-)}[n,k_0 r]$. Without the feedback, the radiative conditions can be used giving negligibly small corrections to the result obtained below. Note that $j^{(-)}[n,k_0 a_d]$ in the expressions of the fields on the outside surface of a particle can be replaced by an approximate value because $k_0 a_d << 1$.

The coefficients $\kappa_{n,m}^{in}$, $\kappa_{n,m}^{out}$ and $q_{n,m}^{in}$, $q_{n,m}^{out}$ of the induced field inside and outside of the dust particle can be determined by matching tangential components of the total $E_{cav} + E_{ind}$, $H_{cav} + H_{ind}$ outside of the particle to the induced field E_{ind}, H_{ind} inside of the particle at $r = a_d$. In the lowest order over the radius $r = a$ it is suffice to take into account only $n = 1$ and $n = 2$ modes.

The matching can be done for each (n,m) mode and for TM and TE modes separately. In the approximation of Eq. (21), the matching conditions give

$$\kappa_{n,m}^{out} = c_{n,m} (\frac{\mu_0 \epsilon}{2})^{2n+1} \frac{(n+1)\Gamma[-n+1/2]}{n\Gamma(n+3/2)}, \quad (28)$$
$$q_{n,m}^{out} = d_{n,m} (\frac{\mu_0 \epsilon}{2})^{2n+1} \frac{\Gamma[-n+1/2]}{\Gamma(n+3/2)}\, h_n(p), \quad (29)$$

where

$$h_n(p) = \frac{n j_n[(1+i)p] - (1+i)p j_n'[(1+i)p]}{(1+n) j_n[(1+i)p] + (1+i)p j_n'[(1+i)p]}, \quad (30)$$

and the prime denote derivative over the argument.

The amplitudes inside of the dust particle are

$$\kappa_{n,m}^{in} = \frac{(2n+1)\sqrt{\pi}}{2n\Gamma(n+3/2) j_n[(1+i)p]} (\frac{\mu_0 \epsilon}{2})^n c_{n,m},$$
$$q_{n,m}^{in} = \frac{(2n+1)\sqrt{\pi}}{2\Gamma(n+3/2)((1+n) j_n[(1+i)p] + (1+i)p j_n'[(1+i)p])} (\frac{\mu_0 \epsilon}{2})^n d_{n,m}. \quad (31)$$

where we use notations

$$p = \frac{a_d}{\delta}, \quad \epsilon = \frac{a_d}{b}, \quad \mu_0 = k_0 b. \tag{32}$$

Calculations of induced fields and force on the dust particle is straightforward, but tedious. We give here the final results for the longitudinal F_z and transverse F_ρ (in respect to the beam axes) components of the force.

The force is the sum of contributions from the magnetic and electric fields taken on the inside surface of the dust particle,

$$F^E = \frac{\pi a^2}{4\pi} \int do\{\hat{r}(E_r E_r^* - E_\beta E_\beta^* - E_\psi E_\psi^*) + \hat{\beta}(E_\beta E_r^* + c.c.) + \hat{\psi}(E_\psi E_r^* + c.c.)\}, \tag{33}$$
$$F^H = \frac{\pi a^2}{4\pi} \int do\{\hat{r}(H_r H_r^* - H_\beta H_\beta^* - H_\psi H_\psi^*) + \hat{\beta}(H_\beta H_r^* + c.c.) + \hat{\psi}(H_\psi H_r^* + c.c.)\}.$$

Here $do = \sin\beta d\beta d\psi$ and Eq.(19) has to be substituted for the unit vectors $\hat{r}$, $\hat{\beta}$, and $\hat{\psi}$ before integration. Expanding over $\delta/b \ll 1$ and $a_d/b \ll 1$ and retaining the linear terms, but allowing the arbitrary ratio $p = a_d/\delta$, we get after the integration that $F^{(E)}$ is of the order of ϵ^2 and can be neglected.

The magnetic field contribution defines the transverse and longitudinal force in respect to the cavity axes:

$$F_\rho = (\hat{R}.F^H)\sin\alpha + (\hat{\alpha}.F^H)\cos\alpha,$$
$$F_z = (\hat{R}.F^H)\cos\alpha - (\hat{\alpha}.F^H)\sin\alpha. \tag{34}$$

Calculations give

$$F_\rho = E_0^2 \frac{a_d^3}{b} [-\frac{c_\rho}{\mu^5 d(\mu)} \cos^2(\alpha) + \frac{s_\rho}{\mu^5 d(\mu)} \sin^2(\alpha)] \sin(\alpha),$$
$$c_\rho = \frac{27}{16}\mu_0(\mu cos\mu - \sin\mu)^2[4j_1((1-i)p)j_1((1+i)p) + 3p(1-i)j_1((1+i)p)j_1'((1-i)p) +$$
$$3(1+i)pj_1((1-i)p)j_1'((1+i)p) + 4p^2 j_1'((1-i)p)j_1'((1+i)p)],$$
$$s_\rho = \frac{9}{16}\mu_0(\mu cos\mu - \sin\mu)\{2j_1((1-i)p)j_1((1+i)p)[6(\mu cos\mu - \sin\mu) +$$
$$8\mu^2 \sin\mu] + [(1-i)pj_1((1+i)p)j_1'((1-i)p) + c.c.](9(\mu cos\mu - \sin\mu) + 8\mu^2 \sin\mu) +$$
$$2j_1'((1-i)p)j_1'((1+i)p)(6p^2(\mu cos\mu - \sin\mu) + 4p^2\mu^2 \sin\mu)],$$
$$d(\mu) = |(1+i)j_1((1-i)p) + pj_1'((1-i)p)|^2. \tag{35}$$

$$F_z = E_0^2 \frac{a_d^3}{b} \frac{c_z}{\mu^5 d(\mu)} \sin^2(\alpha)\cos\alpha,$$

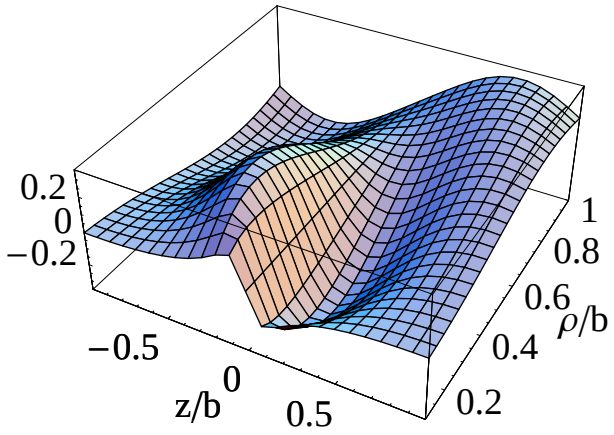

Figure 5: The longitudinal force F_z in units of $E_0^2 a_d^3/b$ for $p = 0.1$.

$$c_z = \frac{9}{8}\mu_0(\mu cos\mu - \sin\mu)\,\{2j_1((1-i)p)j_1((1+i)p)\,[6(\mu cos\mu - \sin\mu) + 4\mu^2\sin\mu] +$$
$$p[(1+i)j_1((1-i)p)j_1'((1+i)p) + c.c.]\,[9(cos\mu - \sin\mu) +$$
$$4\mu^2\sin\mu] + 2p^2 j_1'((1-i)p)j_1'((1+i)p)\,[6(cos\mu - \sin\mu) + 2\mu^2\sin\mu]\}. \quad (36)$$

Result for F_z in the units of $E_0^2 a^3/b$ is shown in Fig. (5) for $p = 0.1$ and (6) for $p = 5.0$, respectively, as function of the dimensionless $z/b = (R/b)\cos(\alpha)$ and $\rho/b = (R/b)\sin(\alpha)$.

The transverse F_ρ is focusing. It is shown in Fig. (7) for $p = 0.1$ and (8) for $p = 5.0$. The azimuthal force $F_\phi = 0$.

The dust particle can be stable in both longitudinal and transverse directions. Dependence on the ratio of the dust particle radius to the skin depth is illustrated in Fig. (9). It is worth noting that since small ρ can be suppressed by a centrifugal force at a nonzero angular momentum $a_d < \delta$, then particles are more likely to be trapped.

The force acting on a dust particle is proportional to a_d^3 if $a_d \simeq \delta$. Because the mass of the particle also scales as a^3, the frequency of small particle oscillations around equilibrium in this case is independent on a_d.

The ohmic losses are proportional to the energy flux to the particle

$$\frac{dU}{dt} = \frac{\pi c a^2}{32\pi}\int \sin\beta d\beta d\psi\{E_\beta H_\psi^* - E_\psi H_\beta^* + c.c.\}. \quad (37)$$

Calculations give

$$\frac{dU}{dt} = cE_0^2\frac{a_d^3}{b}\,\frac{g_u}{\mu^4 d(\mu)}\sin^2(\alpha),$$

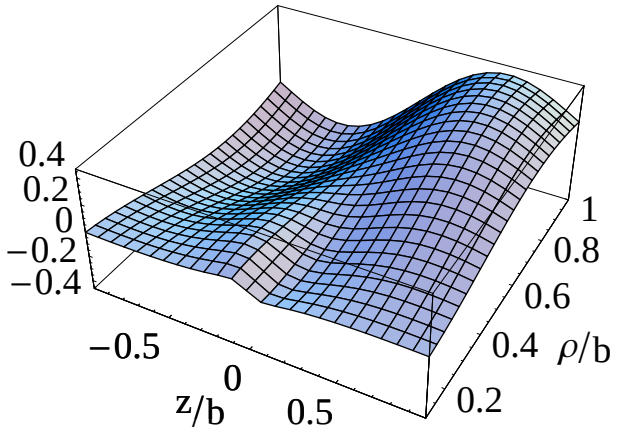

Figure 6: The same as in Fig. (5) with $p = 5.0$.

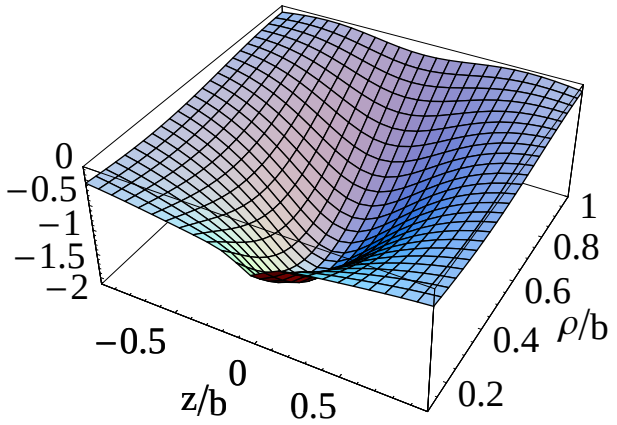

Figure 7: The transverse force F_ρ in units of $E_0^2 a_d^3/b$ for $p = 0.1$.

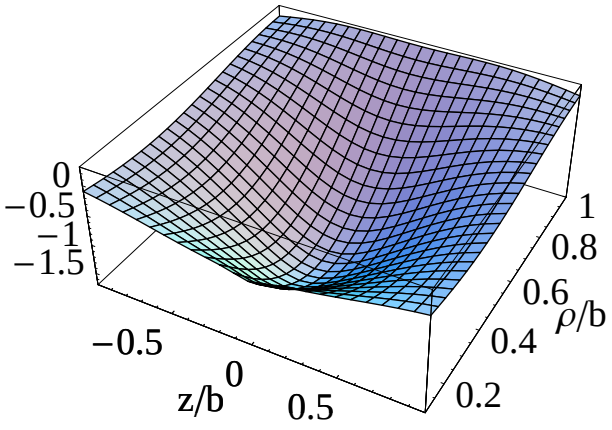

Figure 8: The same as in Fig. (7) with $p = 5.0$.

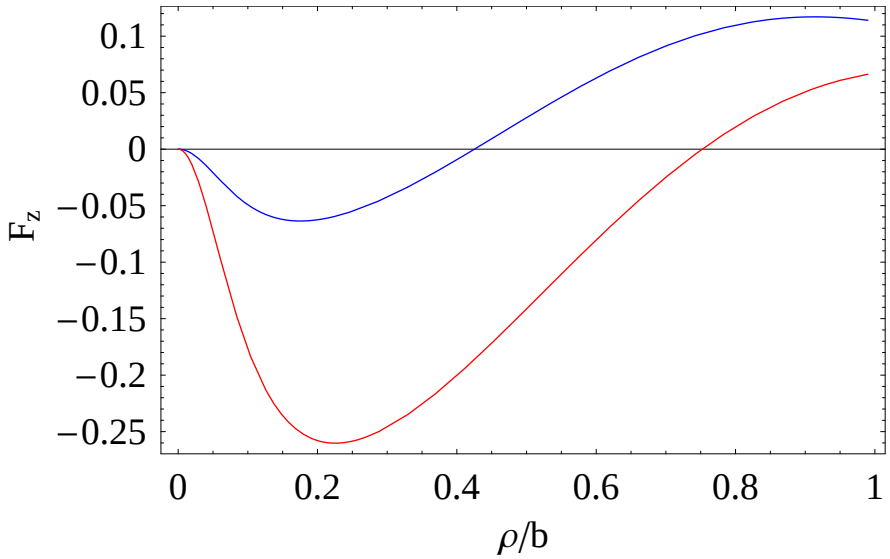

Figure 9: Dependence of the longitudinal force F_z on the parameter $p = a_d/\delta$. F_z is calculated at $z/b = 0.1$ The red and blue curves for $p = 0.1$ and $p = 5.0$, respectively. Transverse stability corresponds to $F_z < 0$.

$$g_u = \frac{27}{64}\mu_0 p\,(\mu cos\mu - \sin\mu)^2\,\{(1+i)j_1((1+i)p)j_1'((1-i)p) + c.c.\}. \qquad (38)$$

For large $p \gg 1$, $g_u \propto 1/p$.

The energy flux can be compared with the energy loss to radiation $dU/dt = \sigma_{SB}T^4 4\pi a^2$, where $\sigma_{SB} = 5.6\,10^{-8}\ W/(m^2K)$ is the Stefan-Boltzmann constant. The equilibrium defines the temperature T. Taking $b = 3.5$ cm, and $E_0 = 1.5$ MV/m, we get $T = 281\,(a^2/\delta)^{1/4}\,K$, where a_d and δ are in μm. The temperature scales proportional to the particle radius $\sqrt{a_d}$ and is larger for large particles with large conductivity. Therefore, there is a trade-off between the stability of particles and the equilibrium temperature. Apparently, additional heating by the field emission electrons is essential to achieve high temperature required for the glowing.

4 Conclusion

The balance of a centrifugal and ponderomotive forces can explain stable motion of a charged particle in a multi-cell RF cavity. Although the RF trapping may be of interest by itself, our main motivation is related to the observation of the light emitting filaments in superconducting RF cavities. Light cannot be caused by the dipole radiation of slow motion of the charged particles, and the particles cannot be stable in a single-cell cavity. The dust particle seems to be a much better candidate causing light emitting filaments.

The light radiated by the filament can be the result either of collisions of a trapped particle with a residual gas or emitted by a hot trapped dust particle. In the experiment [1] the filament radiation has always been observed with the field emission break downs. Because there have always been a lot of electrons at such conditions, but the filaments observations are relatively rare, we believe that the dust, not the electrons, is the source of radiation. As it is described in the mechanical breakup model, when the force due to the intense surface field at the sharp tip on the wall exceeds the tensile strength of the metal, a fragment of the tip may break loose [12]. The angular distribution of the fragments is very broad and, therefore, a fragment can be ejected with the initial angular moment as it is required by our model. The question we address here is, mostly, whether a dust particle can be stable in a single cell RF cavity. We have found that the polarization of the particle can lead to stable motion both longitudinally and transversely. Small (compared to the skin depth at RF frequency) particles have a better chance to be trapped. The skin depth for niobium at 1.5 GHz is of the order of $5\mu m$ and $1\mu m$ particles can be easily produced in the breakdown. The ohmic losses can cause heating of a particle balanced by thermal radiation. Our estimate shows that the equilibrium temperature due to this mechanism, at least, for small particles, is too low. Bombardment by field emission electrons from the remaining tip may produce additional heating. The power of the field emission current is sufficient to heat up (and even vaporize) the micro-particle. It is important that the hot micro-particle can emit electrons acquiring a large positive charge producing condition for particle trapping. The charge of a trapped particle is given by the balance of the ionization

by the field emission electrons from the wall and thermal losses of electrons by the dust particle. The life time of the dust particle depends whether the temperature exceeds the melting point and can be quite large. All these processes are not much different from the processes defining dynamics of the temperature, charge, and lifetime of a dust particles [9].

5 Acknowledgments

The authors thank M. Sullivan and D. Fryberger for having drawn our attention to this interesting topic. Work supported by Department of Energy contract DE–AC02–76-SFO0515.

References

[1] J.R. Delayen, J. Mammosser, "Light emission phenomena in superconducting niobium cavities", Proceedings of the 1999 Particle Accelerator Conference, New York, 1999, p.925.

[2] A.B. Gaponov, and M.A. Miller, "Potential wells for charged particles in a high-frequency electromagnetic field", JETP, 1958, v. 34, pp. 242-243

[3] A.W. Chao, "Particle trapping with an RF cavity", SLAC -PUB-7072, 11/1995

[4] D.Fryberger, "'A small particle model as a possible explanation of recently reported cavity lights"', Nuc. Inst.and Meth. in Physics Research A,459 (2001).

[5] P. A. Anthony, J.L. Delayen, et al, "Experimental studies of light emission phenomena in superconducting RF cavities", SLAC-PUB-13664.

[6] B. M. Bolotovskii, A. V. Serov, "Details of the motion of charged nonrelativistic particles in a variable field", UFN, 1994, Volume 164, Number 5, 545547 (in Russian).

[7] F. Zimmermann, PEP-II AP Note 8-94, May 1994.

[8] F. Zimmermann, J. Seeman, M. Zolotorev, SLAC-PUB-6788, June 1995.

[9] S. Heifets, Qing Qin, M.Zolotorev, "Life of the dust macro-particles in storage rings", Phys. Rev. ST Accel.Beams. 8:061002, 2005

[10] Qing Qin, (BEPC, Beijin), Private communication

[11] A.V.Novokhatsky, "Computer simulations of radiation field dynamics in accelerating structures", Preprint INP 82-157, 1982.

[12] P.B. Wilson, "A Theory for the RF Surface Field for Various Metals at the Destructive Breakdown Limit", 12th workshop on Advanced Accelerator Concepts, AIP Conference Proceedings 877, 27 (2006); doi: 10.1063/1.2409118; describing Norem's mechanical breakup model.

[13] L. Landau, E. Lifshitz, "'Electrodynamics of continuous media", Pergamon Press, Oxford, 1960

[14] J.A. Stratton, "'Electro-Magnetic Theory"', McGRAW-HILL BOOK COMPANY, New York and London, 1941.

6 Appendix 1

The amplitudes of the eigenmodes of the RF field of the cavity at the location R, α are given by the following expressions (where $\mu = k_0 R$):

$$
\begin{aligned}
c_{2,2} &= \frac{5\cos\alpha}{8\mu^4}\,(3\mu\cos\mu - (3-\mu^2)\sin\mu),\\
c_{2,1} &= -\frac{5\sin\alpha}{12\mu^4}(\mu(-6+\mu^2)\cos\mu + 3(2-\mu^2)\sin\mu),\\
c_{2,0} &= -\frac{5\cos\alpha}{2\mu^4}\,(3\mu\cos\mu - (3-\mu^2)sin\mu),\\
c_{2,-1} &= \frac{5\sin\alpha}{2\mu^4}(\mu(-6+\mu^2)\cos\mu + 3(2-\mu^2)\sin\mu),\\
c_{2,-2} &= \frac{15\cos\alpha}{\mu^4}(3\mu\cos\mu + (-3+\mu^2)\sin\mu),\\
c_{1,1} &= \frac{3\cos\alpha}{2\mu^3}(\mu\cos\mu - \sin\mu),\\
c_{1,0} &= \frac{3\sin\alpha}{2\mu^3}(\mu\cos\mu + (-1+\mu^2)\sin\mu),\\
c_{1,-1} &= \frac{3\cos\alpha}{\mu^3}(-\mu\cos\mu + \sin\mu).
\end{aligned}
\tag{39}
$$

$$
\begin{aligned}
d_{2,2} &= \frac{5\sin\alpha}{24\mu^3}\,(3\mu\cos\mu - (3-\mu^2)\sin\mu),\\
d_{2,1} &= d_{2,0} = d_{2,-1} = 0\\
d_{2,-2} &= -\frac{5\sin\alpha}{\mu^3}(3\mu\cos\mu + (-3+\mu^2)\sin\mu),\\
d_{1,1} &= \frac{3\sin\alpha}{4\mu^2}\,(\mu\cos\mu - sin\mu),
\end{aligned}
$$

$$d_{1,0} = 0,$$
$$d_{1,-1} = \frac{3\sin\alpha}{2\mu^2}(\mu\cos\mu - \sin\mu). \tag{40}$$

Note that $c_{1,m}$ are related to the rf components Eq. (17),

$$2c_{1,1} = -c_{1,-1} = i\frac{E^R_{cav}}{E_0}, \quad c_{1,0} = i\frac{E^\alpha_{cav}}{E_0}$$
$$2d_{1,1} = d_{1,-1} = -\frac{H^\phi_{cav}}{E_0}. \tag{41}$$

7 Appendix 2

Here we show that the cavity fields do not contribute to the force acting on the dust particle. Let us start with Eq. (16)

$$F_i = \int \frac{dS}{8\pi}\hat{r}_j[\mathrm{E}_i\mathrm{D}_j + \mathrm{D}_i\mathrm{E}_j - \delta_{i,j}\mathrm{E.D} + (\mathrm{E},\mathrm{D}) \to (\mathrm{H},\mathrm{B})], \tag{42}$$

where the integral is understood as taken over the outer surface of the dust particle assuming that the fields are the fields of the cavity Eq. (17). Expanding fields around the center of the particle, we get in the linear approximation over a_d

$$\mathrm{E}_j(R_0 + a_d\hat{r}) = \mathrm{E}_j(R_0) + a_d(\hat{r}.\nabla)\,\mathrm{E}_j(R_0), \tag{43}$$

and similar expressions for H. Here $\hat{r}$ is the unit radial vector, and ∇ denotes gradient in the cavity c.s. The surface integral gives

$$\int dS\hat{r}_i = 0, \quad \int dS\hat{r}_i\hat{r}_j = \frac{4\pi a_d^2}{3}\,\delta_{i,j}. \tag{44}$$

After substituting $\mathrm{E}_i = E_i e^{-i\omega_0 t} + c.c.$ and averaging over time the force takes the form

$$F_i = \frac{a_d^3}{3}\left[\nabla_j(E_iE_j^* + E_jE_i^*) - \nabla_i(E.E^*) + (E \to H)\right]. \tag{45}$$

Using Maxwell equations for the cavity fields $\nabla_j.E_j = 0$, $\nabla \times E = ik_0H$,$\nabla \times H = -ik_0E$, and identity

$$E_j^*(\nabla_jE_i - \nabla_iE_j) = ik_0(H \times E*)_i, \quad H_j^*(\nabla_jH_i - \nabla_iH_j) = -ik_0(E \times H*)_i, \tag{46}$$

we get

$$F = \frac{a_d^3}{6}\left[ik_0(H \times E*) - ik_0(E \times H*) + c.c.\right] = 0. \tag{47}$$

Therefore, the force is defined only by the induced fields.